Effect of Fengycin, a Lipopeptide Produced by *Bacillus subtilis*, on Model Biomembranes

Magali Deleu,* Michel Paquot,* and Tommy Nylander†
*Unité de Chimie biologique industrielle, Faculté universitaire des Sciences agronomiques de Gembloux, B-5030 Gembloux, Belgium; and †Physical Chemistry 1, Lund University, Center for Chemistry and Chemical Engineering, S-221 00 Lund, Sweden

ABSTRACT Fengycin is a biologically active lipopeptide produced by several *Bacillus subtilis* strains. The lipopeptide is known to develop antifungal activity against filamentous fungi and to have hemolytic activity 40-fold lower than that of surfactin, another lipopeptide produced by *B. subtilis*. The aim of this work is to use complementary biophysical techniques to reveal the mechanism of membrane perturbation by fengycin. These include: 1), the Langmuir trough technique in combination with Brewster angle microscopy to study the lipopeptide penetration into monolayers; 2), ellipsometry to investigate the adsorption of fengycin onto supported lipid bilayers; 3), differential scanning calorimetry to determine the thermotropic properties of lipid bilayers in the presence of fengycin; and 4), cryogenic transmission electron microscopy, which provides information on the structural organization of the lipid/lipopeptide system. From these experiments, the mechanism of fengycin action appears to be based on a two-state transition controlled by the lipopeptide concentration. One state is the monomeric, not deeply anchored and nonperturbing lipopeptide, and the other state is a buried, aggregated form, which is responsible for membrane leakage and bioactivity. The mechanism, thus, appears to be driven mainly by the physicochemical properties of the lipopeptide, i.e., its amphiphilic character and affinity for lipid bilayers.

INTRODUCTION

Fengycin is a biologically active lipopeptide produced by several *Bacillus subtilis* strains (1,2). The structure is composed of a β-hydroxy fatty acid linked to a peptide part comprising 10 amino acids, where 8 of them are organized in a cyclic structure (Fig. 1). This lipopeptide is known to develop antifungal activity against filamentous fungi and to have hemolytic activity 40-fold lower than that of surfactin (1,3,4), another lipopeptide produced by *B. subtilis*. Like most the natural antimicrobial peptides, fengycin likely acts by making the plasma membrane of the target cell more permeable. The molecular mechanism underlying this membrane perturbation is not yet fully understood (5). Due to the complexity of biological systems, the study of interactions between antimicrobial peptides and living cells provides mainly global information about this phenomenon. It is therefore necessary to investigate the interaction of bioactive peptides with different types of model membranes, such as lipid mono- or bilayers, to obtain more precise information about the mechanisms involved.

Only a few studies have been devoted to the characterization of lipid-fengycin interactions. Recently, a monolayer study (5) has demonstrated a concentration-dependent perturbing effect of fengycin on the structural and morphological characteristics of DPPC monolayers. Another work (6) has shown that fengycin organization within a ceramide monolayer is strongly dependent on the environmental conditions (pH, temperature) and fengycin concentration. The major aim of this work is, therefore, to reveal fengycin's mechanism of membrane perturbation via complementary biophysical approaches:

1. The Langmuir trough technique in combination with Brewster angle microscopy is used to obtain information about the penetration properties of fengycin into a lipid monolayer, thus allowing us to directly visualize changes in the monolayer morphology in situ.
2. Ellipsometry is used to investigate the adsorption of fengycin onto supported lipid bilayers. This technique provides time-resolved measurements of changes in the thicknesses and refractive indexes of adsorbed layers and thereby information on the amount on the surface together with structural information (7).
3. Differential scanning calorimetry (DSC) is used to measure the thermotropic properties of lipid bilayer in the presence of fengycin and therefore indirectly provides insight into the organization of molecules within the bilayer.
4. Finally, the cryogenic transmission electron microscopy (cryo-TEM) provides information on the structural organization of lipid/surfactant systems (8). The use of cryo-TEM offers unique possibilities for direct observation of microstructures in terms of both internal structure and morphology. The specimen is prepared with flash freezing in such a way that artifacts due to conventional drying and staining procedures are avoided. This ensures that the structures are maintained in their original state (9).

Membrane models used in this work differ in their complexity (monolayers, supported bilayers, or vesicles) as well as in their nature (dipalmitoylphosphatidylcholine (DPPC)

Submitted June 1, 2007, and accepted for publication November 8, 2007.

Address reprint requests to Magali Deleu, Tel.: 32-81-62-22-32; Fax: 32-81-62-22-31; E-mail: deleu.m@fsagx.ac.be.

Editor: Antoinette Killian.

0006-3495/08/04/2667/13 $2.00

doi: 10.1529/biophysj.107.114090

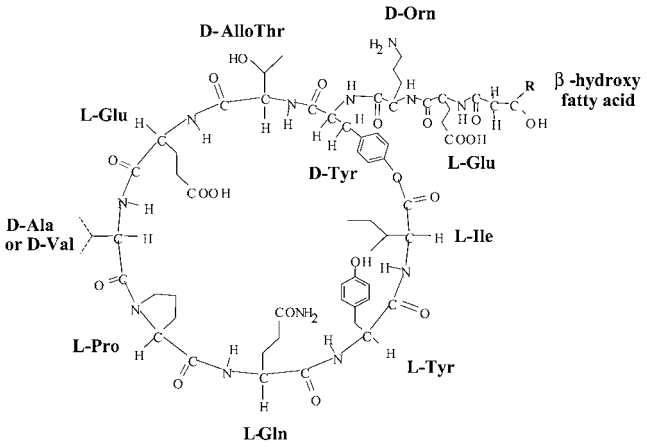

FIGURE 1 Primary structure of fengycin. *R* varies between 11 and 15.

and dioleylphosphatidylcholine (DOPC)) and physical state (fluid or rigid state of the acyl chains). The simplest membrane model is a monomolecular layer of phospholipid spread at the air/water interface. Although monolayers do not reflect the complexity of biological membrane structure, many studies have demonstrated that the monolayer technique is powerful in membrane insertion analysis (10). This system can be considered half of the membrane bilayer. It offers the possibility to simulate what happens when an active molecule, soluble in the extracellular medium, interacts with the membrane surface of target cells. However, the absence of a second membrane leaflet means the reduction of van der Waals interactions, which may be important in natural membranes (11).

Flat bilayers are useful membrane models due to their physical properties and simple geometry. In this study, a supported model membrane is formed via the adsorption of a phospholipid-surfactant mixture onto a silica-water interface, as described by Tiberg et al. (12) and Vacklin et al. (13). This method has been shown to be a flexible and reproducible route to build membrane models with controlled composition. The most complex membrane models used in this study are large unilamellar vesicles (LUV)—bilayer vesicles whose dimension and curvature are of the same order of magnitude as that in natural membranes. The combination of the different lipid membrane models and biophysical techniques provides a comprehensive and detailed analysis of the mechanism of membrane perturbation by fengycin. The results are discussed in relation to the antimicrobial properties of fengycin.

MATERIALS AND METHODS

Materials

Fengycin was produced by fermentation of the *B. subtilis* strain S499 in an optimized culture media as described by Jacques et al. (2) and extracted in a semipreparative scale from the culture medium by solid-phase extraction on Bond Elut C18 (50 g; Varian, Palo Alto, CA) as previously described (14).

The crude extract was applied to a silica gel 60 column (30 × 2.5 cm, 45 g, 250–325 mesh; Merck, Darmstadt, Germany) to use flash chromatography to separate fengycin from surfactin and iturin A, two other types of lipopeptides produced by *B. subtilis*. Fengycin was eluted with chloroform/methanol/water/ethanol (7:3:1.5:3.5, v/v) after elution of surfactin and iturin A. The purity of the sample was verified by infrared spectroscopy, amino acid analysis, analytical reversed-phase high-performance liquid chromatography (HPLC), and matrix-assisted laser desorption/ionization time-of-flight spectrometry. Fengycin is composed of two isoform compounds (isoform A with D-Ala and isoform B with D-Val; Fig. 1), each of them containing fatty acid side chains of variable length.

DPPC (+99%), from Sigma (St. Louis, MO), and DOPC, from Avanti Polar Lipids (Alabaster, AL), were used without further purification. HPLC chloroform (SDS, Peypin, France) and methanol (Merck) of analytical grade were used as spreading solvents. β-D-dodecyl-maltoside was purchased from Sigma at 99% purity.

Preparation of DPPC unilamellar vesicles

Liposomes were prepared as described by Tyteca et al. (15). Briefly, an appropriate amount of DPPC stock solution dissolved in chloroform/methanol (2:1, v/v) was dried in a round-bottom flask under vacuum to obtain a thin film of lipids, which was stored overnight in a vacuum dessicator. The dry lipid film was hydrated for 1 h at 50°C in a 10 mM Tris (Sigma), 150 mM NaCl (Merck) buffer at pH 7.4. The suspension was subjected to five cycles of freezing/thawing to obtain multilamellar vesicles and then extruded to produce LUV via 15 passages on an Avanti Polar Lipids miniextruder composed of one prefilter and two stacked polycarbonate membranes with a pore size of 0.1 μm (polycarbonate filter; Avanti Polar Lipids).

The extruder used was equipped with a heating block, which was set to a temperature between 50°C and 55°C, i.e., significantly above the chain-melting transition temperature of the DPPC. The vesicle shape was verified by cryo-TEM, and measurements by dynamic light scattering show a size of ~100 nm with a narrow size distribution. The lipid concentrations were 1 and 5 mM in the DSC and cryo-TEM experiments, respectively. To reduce the risk for aggregation of vesicles and hydrolysis of the lipids, vesicles were freshly prepared every day and kept (not more than 30 min) at 50°C–55°C before starting the experiment.

Langmuir monolayer penetration

An automatically controlled Langmuir trough (KSV Minitrough, volume = 190 cm^3; KSV Instruments, Helsinki, Finland) equipped with a platinum Wilhelmy plate and placed on a vibration-isolated table was used to study the penetration of fengycin into a DPPC monolayer at the air-subphase interface at different initial surface pressures. The subphase was a 10 mM Tris, 150 mM NaCl buffer at pH 7.4. The temperature was maintained at 30°C ± 0.1°C by external water bath circulation. The temperature of 30°C is close to the chain-melting transition temperature of DPPC and is thus suitable to clearly see the domain formation in a monolayer. At the same time, evaporation from the subphase at this temperature is limited and does not hinder the experiment. The cleanliness of the surface was ensured before each experiment by closing the two symmetrical Delrin barriers and then aspirating the air-liquid interface. The experiment was started only when the surface pressure at maximum compression of the pure subphase was <0.1 mN/m.

DPPC was spread from a 1 mM chloroform/methanol (2:1 v/v) solution on the subphase. At least 10 min was allowed for solvent evaporation from the interface. The spread monolayer was then compressed or expanded symmetrically with the two barriers at a rate of 5.8 $Å^2$ $molecule^{-1}$ $\cdot min^{-1}$ until the desired initial surface pressure was reached with accuracy within 0.1 mN/m. When the DPPC monolayer was stable (i.e., there was no significant change in area), fengycin was injected into the subphase under the DPPC monolayer at a defined position in one step to a final concentration of 27.5 × 10^{-7} M. After injection, the area of the monolayer was kept constant, and the surface pressure increase was recorded with time.

The main experimental problem of recording a curve for a long time is evaporation from the subphase and the risk of contamination, which affects the recorded surface pressure values. Even after 30 min, the subphase level can decrease. Therefore the experiment at $\Pi_i = 21$ mN/m, which was the focus of our study, was conducted with the trough in a closed box with water-saturated air. In the other experiment the plateau value was obtained by extrapolation to infinite adsorption times. The imaging of the monolayer was performed with a Brewster angle microscopy (BAM) Multiskop (Optrel, Berlin, Germany) mounted on the Langmuir trough. Each experiment was repeated at least twice.

Differential scanning calorimetry measurements

The interaction between fengycin and the lipid vesicles were analyzed by DSC using a VP-DSC (MicroCal, Northampton, MA). Differential power between the reference and the sample cell was calibrated electrically by giving a known power pulse to one of the two cells then measuring the resulting change in power. The temperature was calibrated by use of pure paraffin hydrocarbons from MicroCal with precise melting transitions.

After degassing, the liposome suspension was loaded into the sample cell. As reference, 10 mM Tris, 150 mM NaCl buffer at pH 7.4 was used. DSC thermograms were recorded during heating and cooling of the sample from 10°C to 75°C. Initially, two heating rate scans were tested: 1.0°C·min^{-1} and 1.5°C·min^{-1}. The heating rate of 1.0°C·min^{-1} provided the best resolution. After equilibration of the system at the starting temperature for 10 min, the sample was heated to 75°C with a heating rate of 1.0°C·min^{-1}. After a 10 min isotherm, the sample was cooled at the same rate. Thermal cycles were repeated three times to check the reproducibility of the data and to standardize the thermal history of the sample. To avoid the effect of the supercooling phenomenon as discussed by Videira et al. (16), the thermotropic transitions were evaluated from heating curves only.

To determine the thermal midpoint of the transition (T_m), we used the software Origin (OriginLab, Northampton, MA) for DSC. T_m is obtained by fitting our curve data using the Levenberg/Marquardt nonlinear least square method after baseline subtraction and normalization of the data. The onset temperature (T_{onset}) of the transition was determined by linear extrapolation from the low temperature side.

Ellipsometry

Ellipsometry measures the refractive index and thickness of a thin film from the relative amplitude and phase changes of the components of polarized light upon reflection. The rate of data collection in ellipsometry is fast enough to study the evolution of surface structures on a timescale close to seconds and can be used for kinetic studies of surfactant and protein adsorption. The instrument used was a Rudolph Research (Hackettstown, NJ) null ellipsometer, model 43606-200E, which used a xenon arc lamp (OSRAM XBO 75 W/2; OSRAM, Munich, Germany) as a light source (λ = 250–1000 nm). From the ellipsometric angles ψ and Δ, the amplitude, and phase shift upon reflection, we can define the ratio, ρ, between r_s and r_p, which are the reflection coefficients for the s- and p-components of polarized light, respectively:

$$\rho = |r_p/r_s|\exp(\delta_{rp} - \delta_{rs}) = \tan\psi \exp(i\Delta), \qquad (1)$$

where δ_{rp} and δ_{rs} represent the phase shifts upon reflection.

In a typical ellipsometry experiment, the measurement was performed on silicon wafer slides, which were pretreated as described (17,18). The wafers were equilibrated overnight in a 10 mM Tris, 150 mM NaCl buffer adjusted at pH 7.4 with concentrated HCl. The substrate was first characterized by four zone measurements in air and in water after an equilibration period of 30 min, which allowed determination of the complex refractive index of the silicon as well as the refractive index and thickness of the silicon oxide. The substrate optical parameters were on average found to be n_2 (Si) = 5.50–0.25i and $n_1(SiO_2) = 1.49$, d_1 = 270–300 Å.

After flushing the cuvette with 10 mM Tris, 150 mM NaCl, pH 7.4 and equilibration for 30 min, a small amount (10–100 μl) of phospholipid-β dodecyl maltoside stock solution (5.814 g/l with 6:1 w/w surfactant/lipid ratio) solution was introduced into the cuvette with a micropipette. The resulting changes in ψ and Δ were monitored as a function of time until a plateau in both quantities was reached. Then, further changes during the rinsing and the readsorption were recorded until only a very small change resulted from rinsing.

Fengycin in stock buffer (10 mM Tris, 150 mM NaCl, pH 7.4) solution (1–10 mM) was added (1–40 μl,) and the ellipsometric angles were typically monitored over a period of 8–24 h. The resultant data file was converted to thickness, refractive index, and surface excess values by the ellipsometry program, calculating with the Si/SiO_2 four-zone measurements as reference values for the four-layer optical model. The program used de Feijter's approach of calculating the surface excess of an adsorbate as in Eq. 2:

$$\Gamma = [(n - n_0)/(dn/dc)]d, \qquad (2)$$

where n and n_0 are the refractive indexes of the adsorbate and bulk solvent, d is the adsorbed film thickness, and dn/dc is the refractive index increment of the adsorbate, for which a value of 0.148 (18) was used.

The relative errors in thickness estimated from the scatter in the data and the deviation between the reproducibility is rather high (30%–35%) for a small adsorbed amount ($\Gamma < 1.0$ mg/m^2), whereas it is between 2%–7% for $\Gamma > 1.0$ mg/m^2. The error in the adsorbed amount is much smaller: 15% for $\Gamma < 1.0$ mg/m^2 and 0.5%–2% for $\Gamma > 1.0$ mg/m^2.

Cryotransmission electron microscopy

Fengycin stock solution (330 μM–80 mM in 10 mM Tris, 150 mM NaCl, pH 7.4) was added to DPPC unilamellar vesicles prepared as described above to different final concentrations (10 μM, 133 μM, and 2.425 mM). After an incubation for 30 min at room temperature or 50°C, cryo-TEM samples were prepared in a controlled environment vitrification system. The climate chamber temperature was set to 25°C, and the relative humidity was kept close to saturation to prevent evaporation from the sample during preparation. A 5 μl sample drop was placed on a carbon-coated copper grid (2–3 mm diameter) with a hole size of 1–6 μm and thickness up to 500 nm. The drop was gently blotted with filter work to obtain a thin liquid film on the grid. To ensure good spreading of the mostly aqueous samples, the carbon-coated copper grids were first made hydrophilic by a glow discharge treatment, which also rendered them slightly negative. The grid was then rapidly plunged into liquid ethane at −180°C and transferred into liquid nitrogen (−196°C). The vitrified specimens were stored in liquid nitrogen and transferred into a Philips CM120 BioTWIN microscope (Philips, Bothell, WA) equipped with a postcolumn energy filter (Gatan GIF 100; Gatan, Pleasanton, CA) using an Oxford CT 3500 cryoholder and its workstation (Oxford Cryosystems, Oxford, UK). The acceleration voltage was 120 kV, and the working temperature was kept below −180°C. The images were recorded digitally with a charge-coupled device camera (Gatan MSC 791).

RESULTS

Penetration of fengycin into the monolayer model

Addition of fengycin in the subphase underneath a monolayer of DPPC induces a marked increase of surface pressure Π (Fig. 2 *A*), which suggests that fengycin inserts into the lipid monolayer. If the peptide interacted with the lipid headgroups without penetrating into the monolayer, we would not have seen an increase of surface pressure (19). The surface pressure increase with time features four distinct kinetic steps which

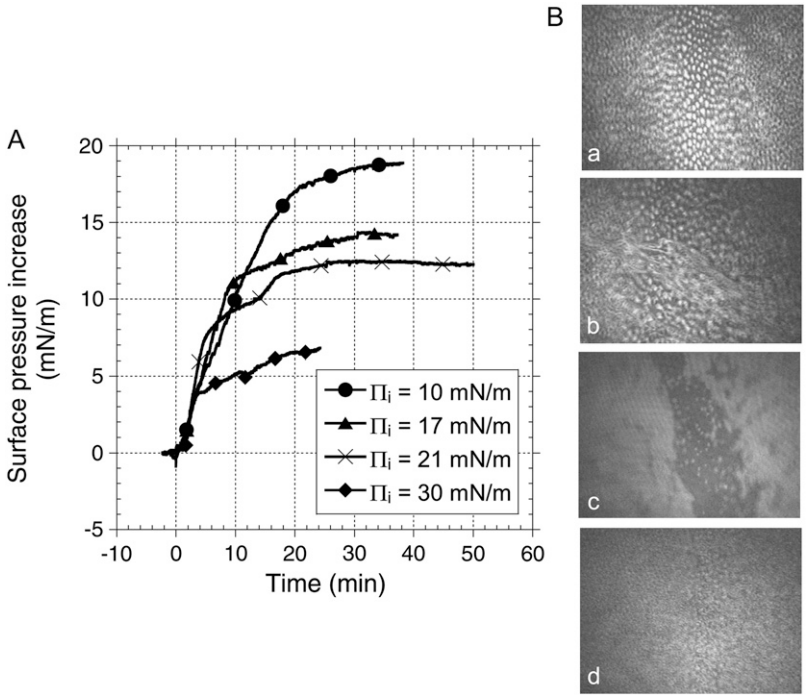

FIGURE 2 (*A*) Surface pressure increase after injection of fengycin (final concentration: 27.5×10^{-7} mM) under a DPPC monolayer previously compressed at a defined initial surface pressure. Numbers in the figure correspond to defined steps discussed in the text. (*B*) BAM images of the interface (*a*) before injection of fengycin and (*b*) 5 min (corresponding to step 1 in *A*), (*c*) 10 min (corresponding to step 2 in *A*), and (*d*) 35 min (corresponding to step 4 in *A*) after injection of fengycin under the DPPC monolayer previously compressed at $\Pi_i = 21$ mN/m. Subphase is a 10 mM Tris, 150 mM NaCl buffer at pH 7.4. Temperature is 30°C.

can be clearly identified in Fig. 2 *A* for the initial surface pressure (Π_i) 17 and 21 mN/m. This change was clearly reflected in the simultaneously recorded BAM images as fast or slow displacement of the domains, respectively. At low and high Π_i, 10 and 30 mN/m, the kinetic steps are not easy to identify from the surface pressure measurements only, but they could be identified from the BAM images.

The BAM images showed more features at a surface pressure of 21 mN/m, as expected since it is at the liquid expanded-liquid condensed phase transition in the isotherm and any effect of fengycin is expected to be larger here. At 30 mN/m, BAM images showing uniform film without domain and penetration of fengycin into the lipid monolayer is expected to give smaller effects. In fact our preliminary images at $\Pi_i = 30$ mN/m showed that penetration of fengycin into the lipid monolayer gave immobile and uniform films, which ultimately seemed to collapse as the films in some experiments became very mobile.

Fig. 2 *B* presents BAM images showing in situ the changes of DPPC monolayer organization corresponding to the four steps of fengycin penetration when $\Pi_i = 21$ mN/m. The first step exhibits a sharp increase of surface pressure, suggesting a rapid insertion of fengycin. When the initial surface pressure is 21 mN/m, well-defined domains can be identified (Fig. 2 *B*, *a*). As fengycin inserts into the monolayer during step 1, the well-separated DPPC domains tend to merge (Fig. 2 *B*, *b*), and the mobility of the layer increases significantly. The corresponding part of the Π versus time curve is more or less independent of the initial surface pressure. In other words, lateral pressure of the lipid monolayer does not seem to affect the initial penetration kinetics if Π_i is smaller than exclusion pressure (Π_{ex}). During the slower increase of Π (step 2), structural changes within the monolayer occur that might involve aggregation of fengycin molecules (Fig. 2 *B*, *c*). Simultaneously an additional adsorption of fengycin molecules occurs which contributes to a second higher pressure increase (step 3). This leads to the formation of large, highly mobile domains and confirms the fluidizing effect of fengycin on the DPPC monolayer (5). During step 4, the lipid-peptide mixed monolayer approaches an equilibrium state. At this stage again, separated domains occur, which are smaller and have different morphology than found in the absence of fengycin (Fig. 2 *B*, *d* compared to Fig. 2 *B*, *a*). This behavior suggests separation into fengycin-rich and DPPC-rich phases.

Fig. 3 summarizes the surface pressure increase induced by fengycin insertion as a function of the initial surface pressure of the DPPC monolayer. The intersection of the regression line with the *x* axis defines the exclusion surface pressure (Π_{ex}), which represents the maximum Π_i permitting the insertion of fengycin into the preformed monolayer. In the DPPC monolayer and under our experimental conditions, $\Pi_{ex} = 41.2$ mN/m.

The adsorption of fengycin at a clean interface (without DPPC monolayer) induces a surface pressure increase of 22.0 mN/m (data not shown). In the presence of DPPC molecules at the interface, fengycin adsorption gives rise to a higher surface pressure increase if initial surface pressure of DPPC monolayer is below 5 mN/m. In other words, fengycin is stabilized at the interface by the presence of DPPC molecules. Interaction between fengycin and DPPC was reported in our previous work (5), where we made a thermodynamic analysis of the miscibility of premixed fengycin/DPPC monolayers. It

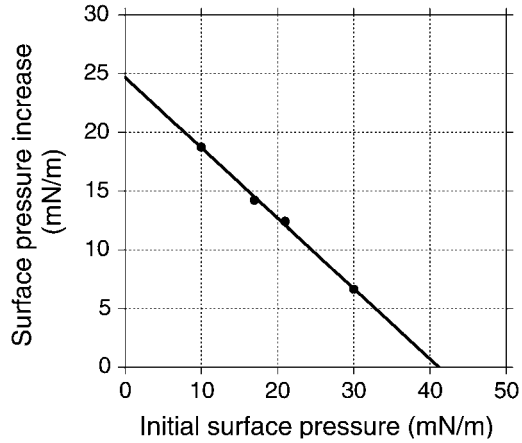

FIGURE 3 Surface pressure increase after injection of fengycin under a DPPC monolayer previously compressed at a defined initial surface pressure. Subphase is a 10 mM Tris, 150 mM NaCl at pH 7.4. Temperature is 30°C. Fengycin is injected into the subphase under the DPPC monolayer at a defined position in one step to a final concentration of 27.5×10^{-7} M. The line represents the linear regression that best fits the experimental data. The intersection with the abscissa estimates the exclusion pressure (Π_{ex}).

suggests that the penetration process does not affect it. As a monolayer is not a relevant model for a biological membrane, further investigations were done on bilayer model systems.

Effect of fengycin on the thermotropic behavior of lipid bilayer models

Both surface film balance and BAM studies indicated phase separation in the presence of fengycin. This was further studied by investigating the thermotropic phase behavior of DPPC unilamellar dispersions (LUV) in mixtures with the lipopeptide by means of DSC. To ascertain the liposome structure after the DSC experiment, cryo-TEM was performed on one sample of pure DPPC vesicles. Fig. 4 shows one of the representative images of this sample, which confirms that the majority of the vesicles are not perturbed by the heating-cooling cycles. It was also noted that repeated temperature scans of the same sample show almost identical thermograms after each heating-cooling cycle (data not shown).

Typical DSC thermograms obtained at the second heating cycle for pure DPPC LUV and for DPPC LUV mixed with fengycin are shown in Fig. 5. The data for the pure DPPC system (Fig. 5 *a*) are in good agreement with those reported elsewhere (16,20,21). DPPC exhibits two endothermic transitions in the range 10°C–75°C. The one centered at 37°C corresponds to the pretransition of a lamellar gel phase to a rippled gel phase ($L_{\beta'}$–$P_{\beta'}$). The existence of pretransition has also been observed in a number of studies (22–24) for unilamellar vesicles at about the same temperatures as in this study. Different models have been applied to predict and explain this pretransition (24). It is generally assumed that it reflects the interactions between the water and the polar head

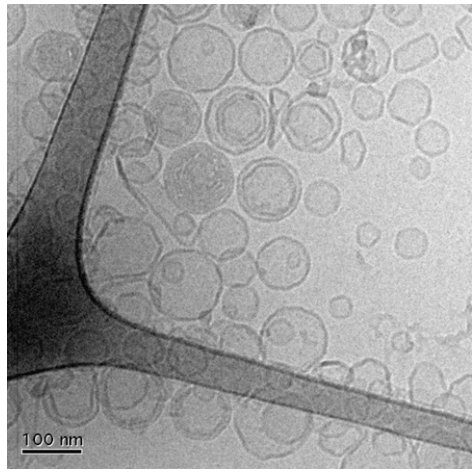

FIGURE 4 Cryo-TEM image of DPPC vesicles after the heating-cooling cycle performed in the DSC experiments.

region of the bilayer (25). This pretransition is observed on the first heating scan of a fresh vesicle preparation and is almost identical after each heating-cooling cycle (data not shown). This is expected, as the cryo-TEM images show that the majority of the vesicles are not perturbed by the heating-cooling cycles. The second transition, called the ''main transition'', is due to the chains melting from a gel phase to a lamellar liquid crystal (P_β–L_α) and is centered at $T_m = 41.7$°C ($T_{onset} = 39.0$°C; Table 1).

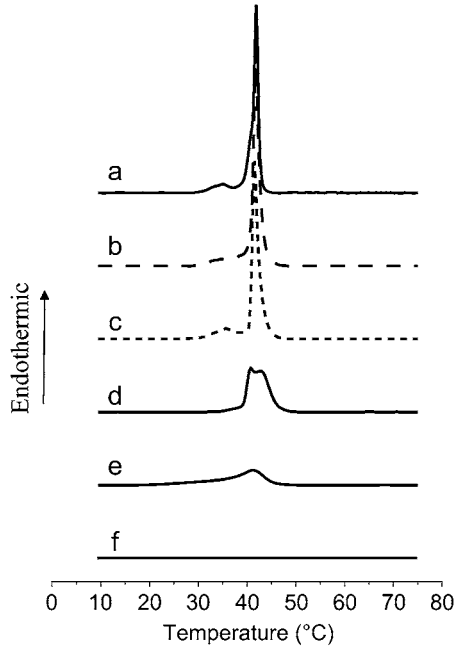

FIGURE 5 Second heating scan of fengycin and/or DPPC vesicles in a 10 mM Tris, 150 mM NaCl buffer at pH 7.4. (*a*) DPPC vesicles 1 mM; (*b*) DPPC/fengycin (300:1), [fengycin] = 3.3 μM; (*c*) DPPC/fengycin (37.5:1), [fengycin] = 25.8 μM; (*d*) DPPC/fengycin (10:1), [fengycin] = 96 μM; (*e*) DPPC/fengycin (2:1), [fengycin] = 0.48 mM; (*f*) fengycin at a concentration of 0.48 mM.

TABLE 1 Effect of fengycin on the thermal midpoint (T_m) and the onset temperature (T_{onset}) of the transition of DPPC LUV (1 mM) as a function of fengycin/lipid molar ratio by using DSC

Lipid/fengycin molar ratio	T_m (°C)	T_{onset} (°C)
1:0	41.7 ± 0.1	39.0 ± 0.5
300:1	41.8 ± 0.1	39.0 ± 0.5
37.5:1	41.5 ± 0.1	39.0 ± 0.5
10:1	40.9 ± 0.1 and 42.9 ± 0.1	36.0 ± 1.0
2:1	41.2 ± 0.1	33.0 ± 1.0

The effect of fengycin on DPPC thermotropic behavior is dependent on the fengycin/lipid molar ratio. At a low fengycin/DPPC molar ratio (3.3×10^{-3}) (Fig. 5 *b* and Table 1), no significant modification of the main transition is observed. However, a slight broadening of the pretransition peak gives evidence of fengycin insertion into the DPPC bilayer. The hydrophilic peptide ring is probably localized close to the polar head of DPPC. Due to its large size, the peptide ring slightly perturbs the organization of this region and consequently modifies its interaction with water. The hydrophobic fatty acid chains are likely oriented parallel to the hydrophobic chains of DPPC, and as they are of the same chain length as that of the lipid, we do not expect that they will significantly affect the arrangement within the hydrocarbon region at the low concentrations used.

Surprisingly, an increase of the fengycin/DPPC molar ratio to 2.6×10^{-2} (Fig. 5 *c*) restores the initial shape of the pretransition peak. A rearrangement of fengycin molecules within the bilayer could achieve a more regular form of the ripple phase. At a fengycin/DPPC molar ratio of 0.1 (Fig. 5 *d*), the phase behavior is dramatically different. The pretransition peak disappears, and the main transition peak is split into two ($T_m = 40.9$°C and $T_m = 42.9$°C; See Table 1). At this concentration, fengycin has a strong effect upon the lipid chain packing. The occurrence of an additional phase transition suggests a lateral phase separation in the liquid-crystalline phase. It is in accordance with other studies (26,27) on analogous systems, namely DPPC in mixture with surfactin, a lipopeptide with a structure similar to that of fengycin. In these articles, it was reported that two transition peaks appeared, which could be attributed to a DPPC-rich domain and a lipopeptide-rich domain. The promotion of lateral phase separation within DPPC bilayer has also previously been reported for insecticide molecules, such as α-endosulfan (16). According to Videira et al. (16) and Jain and Wu (28), a compound that gives a new phospholipid phase transition is likely to be a consequence of an interaction that extends to the polar headgroups of the phospholipids. Thus the additional peak observed for the fengycin/DPPC system indicates that the lipopeptide is located in the membrane close to the lipid-water interface with its hydrophobic chain buried in the apolar region of the bilayer. The results indicate that fengycin has a tendency to self-assemble, which is also suggested by the monolayer studies discussed above.

When the concentration of fengycin is further increased up to a 0.5 fengycin/DPPC molar ratio (Fig. 5 *e*), the thermogram shows only one peak, which is small and broad, suggesting that the extended lamellar phase of DPPC has almost completely disappeared in high fengycin concentration. In other words, insertion of high fengycin concentration perturbs the aligning of the phospholipid acyl chain and globally decreases the cooperativity of the lipid-lipid and lipid-fengycin interaction in the bilayer membrane. According to Bonora et al. (29), who studied the insertion of phthalate esters into DPPC bilayers, the presence of a tail on the low temperature side of the peak suggests that the inserted molecules are soluble in the liquid-crystal phase and distribute preferentially on the boundaries of the fused regions. It is worth noting that the heating thermogram changes during the first scan (data not shown). It means that fengycin requires a fluid physical state of the bilayer to give rise to high perturbation of the DPPC bilayer. The phenomenon is irreversible since the following scans (cooling and heating) are similar.

Adsorption of fengycin onto supported lipid bilayers

Ellipsometry is used to follow the insertion of fengycin into supported phospholipid bilayers versus time by determining the changes in thickness and the adsorbed amount. DPPC and DOPC are used to form the supported bilayer in the gel and fluid states, respectively, at 25°C. The left bottom graphs in Figs. 6 and 7 show the sequential adsorption and rinsing process used to deposit a DPPC and DOPC bilayer, respectively, at the silicon-water interface. In each step the phospholipid is co-adsorbed with β-D dodecyl maltoside (DDM) at a constant phospholipid/DDM molar ratio of 1:6. After each addition, rinsing was performed and the subsequent adsorption was done from a solution with 10 times lower total lipid/surfactant concentration, as described by Tiberg et al. (12) and Vacklin (13).

For DPPC, most of the bilayer-micelle exchange occurs during the first two adsorption steps (from 0 to 110 min), after which only minor changes to the bilayer composition are observed (Table 2). DPPC packs to a much higher final density (adsorbed amount $\Gamma = 6.1$ mg/m^2) than DOPC ($\Gamma = 4.2$ mg/m^2). The final value of thickness (56.9 Å; see Table 2) for the DPPC bilayer is higher than the lipid bilayer thickness (51 ± 3 Å) measured by neutron reflectivity (30). Although, we note that Gandbois et al. (31) reported a 60 ± 2 Å thickness of DPPC bilayer on mica from atomic force microscopy studies, we believe that the work of Vacklin et al. (30) is more relevant, as they used the same method of deposition of the bilayer as this study did. The presence of a water layer on the silica surface has been suggested based on results from studies of similar lipid systems (12,32) and could explain this discrepancy in terms of bilayer thickness. However, recent neutron reflectivity data do not indicate a water layer (13).

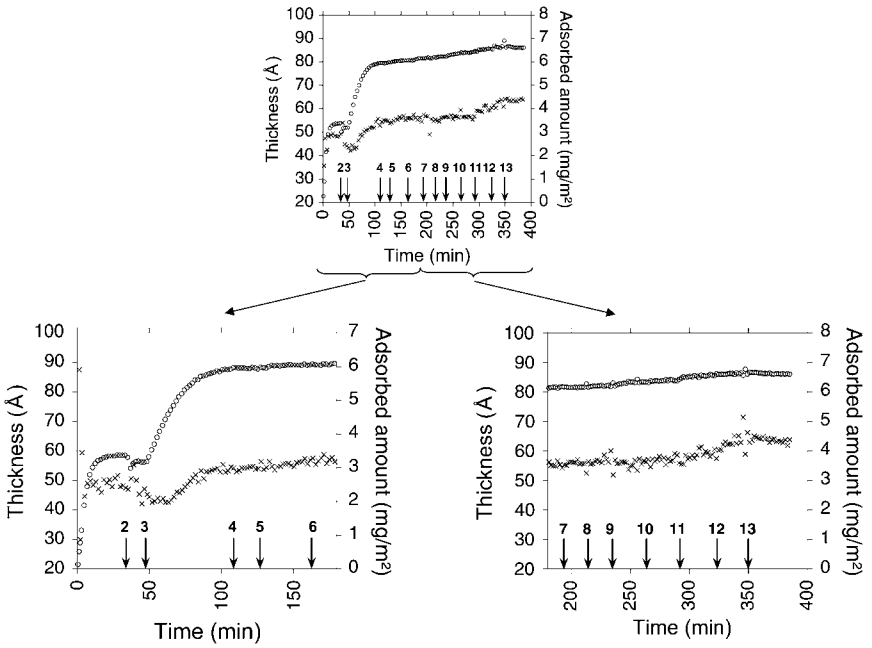

FIGURE 6 Upper graph: Adsorbed amount (*open circles*) and layer thickness (*crosses*) as a function of time for the DPPC/fengycin system. Bottom graphs: magnification of the interesting part of the experiment. (*Left*) Formation and stabilization of the bilayer. Arrows indicate the point at which the composition of the solution was changed. At 0 min, adsorption from 0.114 g/l of DDM/DPPC, (*2*) rinsing with Tris-NaCl, (*3*) adsorption from 0.0114 g/l of DDM/DPPC, (*4*) rinsing with Tris-NaCl, (*5*) adsorption from 0.00114 g/l of DDM/DPPC, (*6*) rinsing with Tris-NaCl. (*Right*) Effect of the increasing fengycin concentration. Arrows indicate the point at which fengycin is injected in the cuvette. Final concentration of fengycin in the cuvette is (*7*) 0.2 μM, (*8*) 2 μM, (*9*) 10 μM, (*10*) 20 μM, (*11*) 100 μM, and (*12*) 180 μM.

We believe that the discrepancy between our value and that of Vacklin et al. (30) is mainly because ellipsometry also is sensitive to optical anisotropy in the layer, which our model does not take into account. This will affect mainly the initial values but not the relative changes observed. Such anisotropy will be more significant for DPPC, which have crystalline chains, as we previously reported for phospholipids at the oil-water interface (33). In the case of DOPC, the evolution of the thickness and adsorbed amount follows that presented by Vacklin (18). In the last addition and rinsing cycle, the surface excess and thickness change by only a small percentage. The final values of thickness (40.5 Å; Table 2) and surface excess (4.2 mg/m^2) suggest the formation of a well-defined DOPC bilayer and are in good agreement with the values

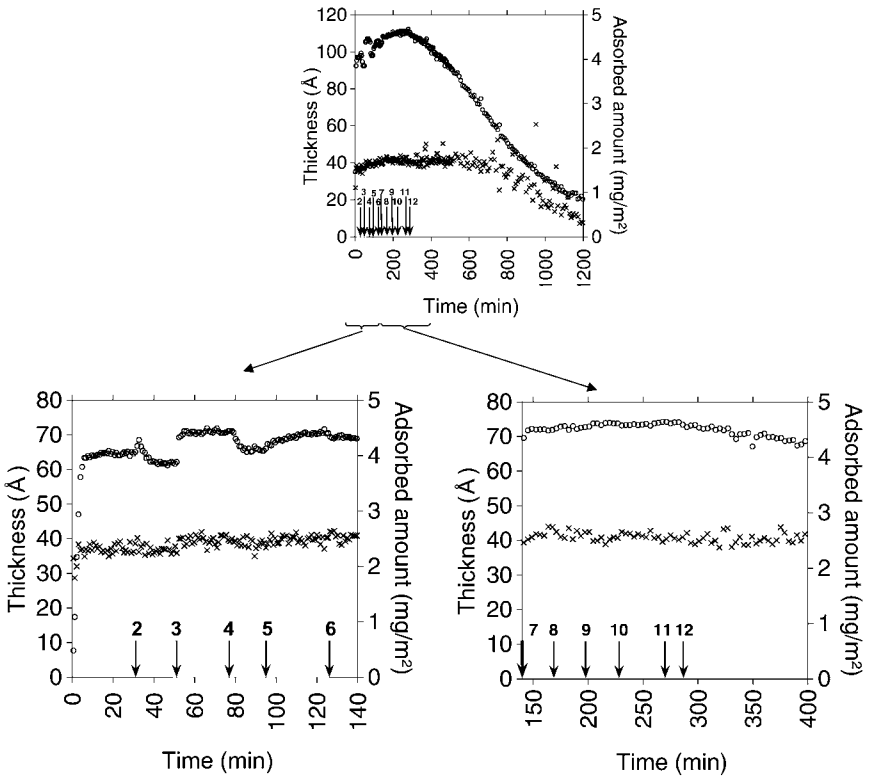

FIGURE 7 (*Upper graph*) Adsorbed amount (*open circles*) and layer thickness (*crosses*) as a function of time for the DOPC/fengycin system. (*Lower graphs*) Magnification of the interesting part of the experiment. (*Left*) Formation and stabilization of the bilayer. Arrows indicate the point at which the composition of the solution was changed. At 0 min, adsorption from 0.114 g/l of DDM/DOPC, (*2*) rinsing with Tris-NaCl, (*3*) adsorption from 0.0114 g/l of DDM/DOPC, (*4*) rinsing with Tris-NaCl, (*5*) adsorption from 0.00114 g/l of DDM/DOPC, (*6*) rinsing with Tris-NaCl. (*Right*) Effect of the increasing fengycin concentration. Arrows indicate the point at which fengycin is injected in the cuvette. Final concentration of fengycin in the cuvette is (*7*) 0.2 μM, (*8*) 2 μM, (*9*) 10 μM, (*10*) 20 μM, (*11*) 100 μM, and (*12*) 180 μM.

TABLE 2 Adsorbed layer thickness (*d*) and adsorbed amount (Γ) onto silicon wafer support subsequent to solution changes in the case of DPPC/fengycin and DOPC/fengycin systems

		DPPC bilayer		DOPC bilayer	
		d (Å)*	Γ (mg/m^2)*	*d* (Å)*	Γ (mg/m^2)*
Formation of bilayer	0.114 g/l DDM-PL†	49.4	3.4	36.7	4.0
	Rinsing‡	44.6	3.2	37.2	3.9
	0.0114 g/l DDM-PL†	53.9	6.0	39.5	4.5
	Rinsing‡	54.5	6.0	38.7	4.1
	0.00114 g/l DDM-PL†	56.8	6.1	40.6	4.2
	Pure bilayer after rinsing‡	56.9	6.1	40.5	4.2
Effect of increasing fengycin concentration	0.2 μM	56.8	6.2	41.3	4.5
	2 μM	56.7	6.2	41.2	4.6
	10 μM	56.4	6.4	40.6	4.6
	20 μM	56.9	6.4	40.7	4.6
	100 μM	60.5	6.4	41.0	4.6
	180 μM	63.8	6.5	11.0	0.9

The values are extracted from Figs. 6 and 7.

*The relative errors in thickness (*d*) are rather high (30%–35%) for small adsorbed amounts (Γ < 1.0 mg/m^2), decreasing rapidly to values around 2%–7% for Γ > 1.0 mg/m^2. The error in adsorbed amounts is much smaller: 15% for Γ < 1.0 mg/m^2 and 0.2%–0.5% for Γ > 1.0 mg/m^2.

†β dodecyl maltoside, phospholipid.

‡Rinsing with 10 mM Tris, 150 mM NaCl buffer at pH 7.4.

obtained by Vacklin (18), who used the same procedure ($d =$ 39.3 Å and $\Gamma = 4.4$ mg/m^2).

The right bottom graphs in Figs. 6 and 7 present the effect of fengycin on the DPPC and DOPC bilayers integrity, respectively. Whatever the physical state of the lipid bilayer, the adsorbed amount initially increases after injection of fengycin (Table 2). This is a strong indication of fengycin adsorption into the bilayer. The increase of the adsorbed amount is slightly higher for DOPC than DPPC at a given fengycin concentration in the aqueous medium (e.g., at 100 μM $\Delta\Gamma_{DPPC} = 0.3$ mg/m^2, whereas $\Delta\Gamma_{DOPC} = 0.4$ mg/m^2). It indicates that fengycin incorporation is easier when the bilayer is in a fluid rather than in a gel state. This has also been observed for numerous other drugs (34) and detergents (35).

The thickness of the DPPC bilayer increases significantly when fengycin is added at a concentration of 100 μM (Table 2). This suggests that fengycin molecules are not completely embedded within the DPPC bilayer but protrude at least partially in the aqueous medium. Even at a high concentration of fengycin and over a long incubation time (12 h; data not shown), the DPPC bilayer retains its integrity. This is due to the tight packing of DPPC in the bilayer, which hampers deep insertion of fengycin. The thickness of the DOPC bilayer, when the phospholipid bilayer is in a fluid state, is not significantly changed by fengycin addition up to a concentration of 180 μM (Table 2), although the adsorbed amount increases significantly after the first addition. This suggests that below this concentration fengycin inserts more deeply into the DOPC bilayer than it does into the DPPC bilayer.

A decrease of the adsorbed amount is observed directly after adding 180 μM fengycin (Fig. 7 *right side*), whereas a significant reduction of the DOPC bilayer thickness is observed only after 400 min. The reduction of the thickness to an almost zero value demonstrates a complete removal of the DOPC bilayer from the silicon-water interface. The penetration of fengycin and the large polar head compared to the small apolar chain gives a positive spontaneous curvature of the bilayer (36,37) that distorts the bilayer structure. In this respect, fengycin acts as a surfactant and is able to solubilize and remove phospholipid molecules.

Effect of fengycin on the morphology of lipid vesicles

Fig. 8, *a–g* shows cryo-TEM micrographs of DPPC vesicles, fengycin alone, and DPPC vesicles incubated with different concentrations of fengycin for 30 min at a temperature over the chain-melting transition temperature of DPPC. The dark strands in the images are the support grid, and the light areas are the frozen sample film confined within the grid. Vesicles formed by DPPC are mostly unilamellar (Fig. 8 *a*). Since they are vitrified from room temperature, i.e., a temperature below the transition temperature, they exhibit a polyhedral shape with faceted surfaces, as observed by Andersson et al. (38). A cryo-TEM micrograph of fengycin solution at 133 μM exhibits small dots of 4–5 nm diameter on the surface of the supporting grid (Fig. 8 *b*); these are likely to be micelles of fengycin. However, it is not possible to discern the precise size and shape of these aggregates from the cryo-TEM micrograph. Small angle neutron scattering may be useful for this investigation. Similar micelle-like aggregates have previously been observed in the case of DOPC-DDM solutions (13). At high concentration (2.425 mM), these aggregates seem to be associated into rod-like structures (Fig. 8 *c*).

The addition of fengycin onto preformed vesicles is dependent on the fengycin/phospholipid ratio. Three different stages can be distinguished, as suggested by Silvander et al. (8) and Mitchell and Ninham (39) for other small surfactants:

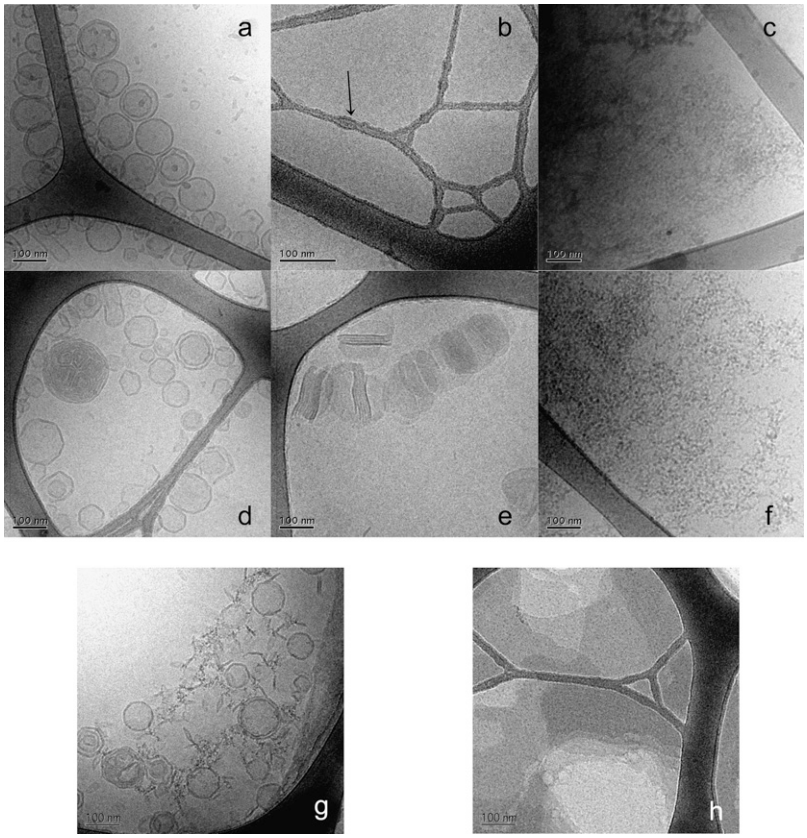

FIGURE 8 Cryo-TEM images (*a*) DPPC vesicles 5 mM; (*b*) fengycin 133 μM, the arrow points out, as an example, a grid border where fengycin micelles are adsorbed; (*c*) fengycin 2.425 mM; (*d*) DPPC/fengycin (500:1), [fengycin] = 10 μM; (*e*) DPPC/fengycin (37.5:1), [fengycin] = 133 μM; (*f*) DPPC/fengycin (2:1), [fengycin] = 2.425 mM. For (*d–f*), fengycin is incubated with DPPC vesicles at 50°C for 30 min. After this time the sample temperature is brought back to room temperature and the vitrification is operated from 25°C. (*g*) DPPC/fengycin (37.5:1), [fengycin] = 133 μM, fengycin is incubated with DPPC vesicles at room temperature for 30 min and the vitrification is operated from 25°C. (*h*) DPPC/fengycin (37.5:1), [fengycin] = 133 μM, fengycin is incubated with DPPC vesicles at 50°C for 30 min, and the vitrification is operated from 45°C.

1. The addition of 0.2 mol % of fengycin (fengycin/phospholipid ratio = 0.002; concentration of fengycin in the system = 10 μM) does not lead to any detectable change in the size or morphology of vesicles (Fig. 8 *d*). However, this does not exclude the possibility that fengycin interacts with the bilayer without causing any major alteration in the bilayer architecture.
2. At a fengycin/DPPC ratio of 0.026 (fengycin concentration = 133 μM), the physical state of the bilayer influences the action of fengycin. The addition of fengycin to DPPC vesicles in a gel state gives rise to open and closed vesicles as well as thread-like micelles (Fig. 8 *g*). However, above the DPPC chain melting transition temperature, flat fragments, composed of perforated lamellar phase, dominate the sample (Fig. 8 *h*). The cooling of the latter sample to room temperature gives rise to disk-like structures (Fig. 8 *e*). Bilayer disks are the same size as the liposomes from which they were derived. This kind of structure has analogies with bicelles and with catanionic disks (40). The formation of a discoidal structure has also been observed when poly(ethylene glycol)-phospholipids are mixed with phosphatidylcholine (41).
3. At a higher fengycin/lipid molar ratio (0.5) (fengycin concentration = 2.425 mM), bilayers are completely disrupted. Entangled thread-like aggregates are observed in the cryo-TEM images. They are suggested to be mixed micelles of fengycin and DPPC. Even if the micrograph does not allow the micelle structure to be properly observed, their existence is assumed on the basis of a recent study (27). In this work, Kell et al. studied the different forms of DMPC-surfactin aggregates, surfactin being another lipopeptide with a structure similar to that of fengycin. At high surfactin molar ratio Kell et al. observed the formation of mixed micelles. Investigation by small angle neutron scattering should be performed on our system to gain a better idea of the size and conformation of the mixed micelles.

DISCUSSION AND CONCLUSION

The main objectives of this study were to investigate the fengycin binding to and/or insertion into a model biomembrane to reveal its perturbing effect and better understand its biological action. Monolayer experiments were used to determine the kinetics of fengycin insertion into a DPPC monolayer. The onset of penetration occurs very quickly, and an equilibrium state is reached after ~30 min, which is more rapid than in the case of a protein (42). The small size of the fengycin peptide part and its strong amphiphilic character facilitate its insertion into the membrane and thus speeds up the process. This information may not only be useful for lung surfactant substitution studies but also give evidence of fengycin penetration into biological membranes from an

aqueous phase. It allows us to confirm that the observed effects with the other techniques are related to the fengycin penetration into the phospholipid film.

The BAM images show that fengycin promotes the merging of the DPPC domains at the initial stages of the penetration process. This kind of behavior was observed for different proteins such as β-lactoglobulin, lysozyme, and β-casein (42). In contrast to the proteins, fengycin insertion leads to a perturbation and partial dissolution of the DPPC condensed domains, which are partially mixed with fengycin. This effect implies an attractive interaction between fengycin and DPPC in the monolayer, which we reported in a previous study of the surface properties of premixed DPPC-fengycin monolayers (5). The high value of exclusion surface pressure, Π_{ex} (41.2 mN/m), observed under the conditions used in this study suggests that fengycin can potentially insert into biological membranes in vivo, for which the surface pressure is estimated to be between 31 and 34 mN/m (11,43).

The results from ellipsometric measurements have confirmed the penetration ability of fengycin into lipid bilayers. These results also highlighted the influence of the phospholipid bilayer's physical state on fengycin binding and insertion. Insertion of fengycin into a fluid-like membrane is easier than it is in a tightly packed bilayer with lipids in the gel state. Consequently, the threshold at which complete bilayer solubilization occurs is lower when the bilayer is in a fluid state. The introduction of the detergent-like fengycin into the bilayer when it is in the gel state is probably the limiting factor for the solubilization process. Cryo-TEM imaging of DPPC vesicles incubated with fengycin at room temperature, therefore, shows intact vesicles. These trends are confirmed by results from other studies (35), which report a slower micellization kinetics for DPPC vesicles in a gel state by Triton-X100. This phenomenon was, as in our study, attributed to the limited (insufficiently deep) introduction of the surfactant into the bilayer.

The overall membrane organization (and particularly the physical state of the lipid component) has also been shown to be a key factor in controlling the membrane activity of nystatin, a polyene antibiotic molecule, as well as its ability to self-assemble within the bilayer (44). The influence of the lipid bilayer state on their solubilization by detergents is physiologically significant because tightly packed liquid-ordered macro- and microdomains exist in biological membranes (45–51). These domains, commonly denoted ''rafts'', have a lipid composition distinctly different from that of the remaining liquid-like (disordered) part of the membrane. They are believed to be rich in lipids with high phase transition temperatures, which tend to be tightly packed and form gel phase bilayers. These include phospholipids bearing relatively long and saturated acyl chains, sphingolipids, and cholesterol (50–55). The formation of liquid-ordered domains is controlled by the ability of the lipids to form close-packed and highly ordered bilayers and to a much lesser extent by specific intermolecular interactions (50).

The mechanism involved in the bilayer solubilization by fengycin can be understood, at least partially, from cryo-TEM and DSC data. Three steps can be distinguished by fengycin concentration and its ratio with respect to the lipid (Fig. 9).

Low fengycin concentration

At low fengycin concentration ($\leq$10 μM, fengycin/lipid molar ratio = 0.002), where the insertion of fengycin does not significantly affect the phospholipid interfacial assembly, fengycin is dispersed as a monomer into the hydrophobic core of the bilayer (Fig. 9 *i*). Its hydrophobic fatty acid chain is probably aligned with the prevailing direction of the phospholipid acyl chains. Thus the DSC thermogram is not affected by the presence of the fengycin. The ellipsometric results suggest that for DPPC the peptide part is likely outside the bilayer and, consequently, does not affect the bilayer structure. The monomeric insertion of fengycin corresponds to the first step of membrane solubilization by a detergent effect (56–59).

Medium fengycin concentration

At medium fengycin concentration (133 μM, fengycin/lipid molar ratio = 0.026), where the bilayer self-assembled structure is affected, fengycin accumulation within the bilayer leads to self-association of fengycin molecules (Fig. 9 *ii*). As the fengycin headgroup has a high relative area with respect to its tail group, the packing parameter concept (36,37) suggests that the thermodynamically most favored aggregate has a positive curvature, e.g., micelle-like structures. At a saturation threshold and a temperature higher than the DPPC transition temperature, large flat fragments are formed. The heating above the chain melting transition temperature initiates a reorganization of the flat structure into flat bilayer disks. This has been demonstrated for other molecules, e.g., lysophospholipids, that also favor micellar structures (60). Fengycin is probably segregated at the edges of DPPC flat disks and forms a rim stabilizing the system. An accommodation of conflicting geometric constraints imposed by the two components and the high tendency of fengycin to self-aggregate are in favor of this mechanism. The presence of amphiphilic molecules in the rim stabilizes the flat disk without any additional cost in bilayer-bending energy (40).

The fact that the main-chain melting transition peak in the DSC thermogram remains at medium fengycin concentration suggests the existence of this disk-like structure, where the fengycin is located at the rim of the disk. Our results are in agreement with the recent report by Sandström et al. (61), who studied disk formation in mixtures of phospholipids and polyethylene glycol phospholipids, where the latter forms micellar-type aggregates. They also found that lipids and conditions that reduce the lipid spontaneous curvature and increase the monolayer bending modulus tend to promote

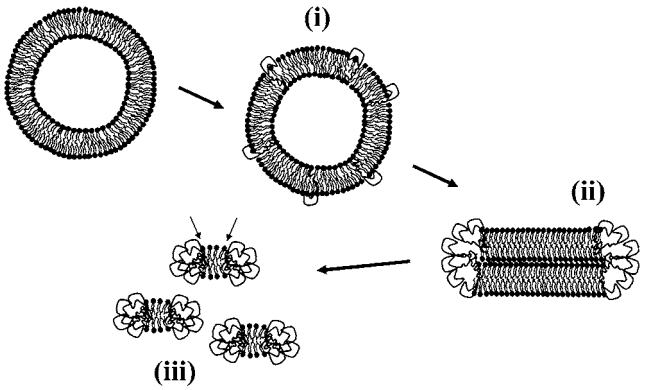

FIGURE 9 Proposed model for the concentration-dependent mechanism of membrane perturbation by fengycin. (*i*), (*ii*), and (*iii*) and arrows: see text for explanation.

formation of discoidal micelles. This effect was found to be enhanced by the reduced lipid/polyethylene glycol lipid miscibility at temperatures below the gel-to-liquid crystalline phase transition temperature. The saturation of the lipid bilayer by fengycin corresponds to the second step of a detergent-like mechanism (57).

High fengycin concentration

At sufficiently high fengycin concentration, the lipid bilayer is completely disrupted into mixed micelles (Fig. 9 *iii*). The subsistence of a (weak) transition peak in DSC suggests the presence of ordered phospholipid hydrocarbon chains, as reported by Funari et al. (62) for $C_{12}E_8$/DPPC mixture at a molar ratio of 1:1. According to Funari et al., the mixture forms a self-assembled structure that might be described as gel-state micelles. A similar model can be suggested in our case. The micelles would be composed of a discoidal cluster of almost pure phospholipids in gel state, the interfacial edge of which is shielded from the surrounding aqueous medium by a semitoroidal collar of fengycin molecules. An outer phospholipid layer is probably perturbed by contact with the surrounding fengycin (See *arrows* in Fig. 9), which explains the less cooperative transition peak observed in DSC.

The effect of fengycin on lipid packing is to some extent comparable to the perturbing properties of surfactant protein C peptide, a pulmonary surfactant, on DPPC monolayer (63). This kind of effect is presumably important in promoting lipid interfacial transfer during the respiratory cycle. This suggests that fengycin may be a candidate to promote or at least initiate transfer of phospholipids into the interface.

To conclude, the mechanism of fengycin action is probably based on a two-state transition controlled by the lipopeptide concentration. One state is the monomeric, not deeply anchored, and nonperturbing lipopeptide, and the other state is a buried, aggregated form, which is responsible for membrane leakage and bioactivity. The mechanism is thus suggested to be driven mainly by the physicochemical properties of the lipopeptide, i.e., its amphiphilic character and affinity for lipid bilayers.

The authors thank Professor P. Thonart and his team for the production of the fengycin by fermentation of the *Bacillus subtilis* strain S499. We are grateful to Gunnel Karlsson for her invaluable help with the cryo-TEM experiments, Marité Cardenas for her help with the ellipsometry experiments, and Prof. Gerd Olofsson and Marc Eeman for useful discussions.

M.D. thanks the Fonds National de la Recherche Scientifique, Belgium for her research associate position and the European Commission for financial support via a Marie Curie Individual Fellowship. T.N. acknowledges support from the Swedish Research Council.

REFERENCES

1. Vanittanakom, N., W. Loeffler, U. Koch, and G. Jung. 1986. Fengycin—a novel antifungal lipopeptide antibiotic produced by Bacillus subtilis F-29-3. *J. Antibiot. (Tokyo).* 39:888–901.
2. Jacques, P., C. Hbid, J. Destain, H. Razafindralambo, M. Paquot, E. De Pauw, and P. Thonart. 1999. Optimization of biosurfactant lipopeptide production from Bacillus subtilis S499 by Plackett-Burman design. *Appl. Biochem. Biotechnol.* 77–79:223–233.
3. Hbid, C. 1996. Contribution à l'étude de la relation entre la structure des lipopeptides de B. subtilis et leurs activités hémolytique et antifongique. PhD thesis. Université de Liège, Belgium.
4. Schneider, J., K. Taraz, H. Budzikiewicz, M. Deleu, P. Thonart, and P. Jacques. 1999. The structure of two fengycins from Bacillus subtilis S499. *Z. Naturforsch [C].* 54:859–866.
5. Deleu, M., M. Paquot, and T. Nylander. 2005. Fengycin interaction with lipid monolayers at the air-aqueous interface—implications for the effect of fengycin on biological membranes. *J. Colloid Interface Sci.* 283:358–365.
6. Eeman, M., M. Deleu, M. Paquot, P. Thonart, and Y. Dufrene. 2005. Nanoscale properties of mixed fengycin/ceramide monolayers explored using atomic force microscopy. *Langmuir.* 21:2505–2511.
7. Zhmud, B., and F. Tiberg. 2005. Interfacial dynamics and structure of surfactant layers. *Adv. Colloid Interface Sci.* 113:21–42.
8. Silvander, M., G. Karlsson, and K. Edwards. 1996. Vesicle solubilization by alkyl sulfate surfactants: a cryo-TEM study of the vesicle to micelle transition. *J. Colloid Interface Sci.* 179:104–113.
9. Edwards, K., J. Gustafsson, M. Almgren, and G. Karlsson. 1993. Solubilization of lecithin vesicles by a cationic surfactant—intermediate structures in the vesicle micelle transition observed by cryo-transmission electron microscopy. *J. Colloid Interface Sci.* 161:299–309.
10. Brezesinski, G., and H. Mohwald. 2003. Langmuir monolayers to study interactions at model membrane surfaces. *Adv. Colloid Interface Sci.* 100–102:563–584.
11. Marsh, D. 1996. Lateral pressure in membranes. *Biochim. Biophys. Acta.* 1286:183–223.
12. Tiberg, F., I. Harwigsson, and M. Malmsten. 2000. Formation of model lipid bilayers at the silica-water interface by co-adsorption with non-ionic dodecyl maltoside surfactant. *Eur. Biophys. J.* 29:196–203.
13. Vacklin, H. P., F. Tiberg, and R. K. Thomas. 2005. Formation of supported phospholipid bilayers, via co-adsorption with beta-D-dodecyl maltoside. *Biochim. Biophys. Acta.* 1668:17–24.
14. Razafindralambo, H., M. Paquot, C. Hbid, P. Jacques, and P. Thonart. 1993. Purification of antifungal lipopeptides by reversed-phase high-performance liquid chromatography. *J. Chromatogr.* 639:81–85.
15. Tyteca, D., A. Schanck, Y. Dufrene, M. Deleu, P. Courtoy, P. Tulkens, and M. Mingeot-Leclercq. 2003. The macrolide antibiotic azithromycin interacts with lipids and affects membrane organization and fluidity: studies on Langmuir-Blodgett monolayers, liposomes and J774 macrophages. *J. Membr. Biol.* 192:203–215.

16. Videira, R. A., M. C. Antunes-Madeira, and V. M. C. Madeira. 1999. Perturbations induced by α-and β-endosulfan in lipid membranes: a DSC and fluorescence polarization study. *Biochim. Biophys. Acta.* 1419: 151–163.

17. Tiberg, F., and M. Landgren. 1993. Characterization of thin nonionic surfactant films at the silica/water interface by means of ellipsometry. *Langmuir.* 9:927–932.

18. Vacklin, H. 2003. Phospholipase A2 action at solid supported phospholipid membranes. PhD thesis. University of Oxford, Oxford, UK.

19. Demel, R. A., Y. London, W. S. M. Geurts van Kessel, F. G. A. Vossenberg., and L. L. M. Van Deenen. 1973. The specific interactions of myelin basic protein with lipids at the air-water interface. *Biochim. Biophys. Acta.* 311:507–519.

20. Blume, A. 1991. Biological calorimetry: membranes. *Thermochim. Acta.* 193:299–347.

21. Tahir, A., C. Gabrielle-Madelmont, C. Betrencourt, M. Ollivon, and P. Peretti. 1999. A differential scanning calorimetry study of the interaction of lasalocid antibiotic with phospholipid bilayers. *Chem. Phys. Lipids.* 103:57–65.

22. Heimburg, T. 1998. Mechanical aspects of membrane thermodynamics. Estimation of the mechanical properties of lipid membranes close to the chain melting transition from calorimetry. *Biochim. Biophys. Acta.* 1415: 147–162.

23. Lichtenberg, D., M. Menashe, S. Donaldson, and R. L. Biltonen. 1984. Thermodynamic characterization of the pretransition of unilamellar dipalmitoyl-phosphatidylcholine vesicles. *Lipids.* 19:395–400.

24. Heimburg, T. 2000. A model for the lipid pretransition: coupling of ripple formation with the chain melting transition. *Biophys. J.* 78:1154–1165.

25. Csiszar, A., A. Bota, C. Novak, E. Klumpp, and G. Subklew. 2002. Calorimetric study of the effects of 2,4-dichlorophenol on the thermotropic phase behavior of DPPC liposomes. *J. Therm. Anal. Calorim.* 69:53–63.

26. Grau, A., J. C. Gómez Fernández, F. Peypoux, and A. Ortiz. 1999. A study on the interactions of surfactin with phospholipid vesicles. *Biochim. Biophys. Acta.* 1418:307–319.

27. Kell, H., J. F. Holzwarth, C. Boettcher, R. K. Heenan, and J. Vater. 2007. Physicochemical studies of the interaction of the lipoheptapeptide surfactin with lipid bilayers of L-α-dimyristoyl phosphatidylcholine. *Biophys. Chem.* 128:114–124.

28. Jain, M. K., and N. M. Wu. 1977. Effect of small molecules on the dipalmitoyl lecithin liposomal bilayer. III. Phase transition in lipid bilayer. *J. Membr. Biol.* 34:157–201.

29. Bonora, S., G. Fini, and B. Piccirilli. 2000. DSC study on the interaction between bis-2-(ethylhexyl) phthalate and other o-phthalic acid esters and dipalmitoyl phosphatidylcholine liposomes. *J. Therm. Anal. Calorim.* 61:731–743.

30. Vacklin, H. P., F. Tiberg, G. Fragneto, and R. K. Thomas. 2005. Composition of supported model membranes determined by neutron reflection. *Langmuir.* 21:2827–2837.

31. Grandbois, M., H. Clausen-Schauman, and H. Gaub. 1998. Atomic force microscope imaging of phospholipid bilayer degradation by phospholipase A2. *Biophys. J.* 74:2398–2404.

32. Johnson, S. J., T. M. Bayerl, D. C. McDermott, G. W. Adam, A. R. Rennie, R. K. Thomas, and E. Sackmann. 1991. Structure of an adsorbed dimyristoylphosphatidylcholine bilayer measured with specular reflection of neutrons. *Biophys. J.* 59:289–294.

33. Benjamins, J.-W., K. Thuresson, and T. Nylander. 2005. Formation of a liquid crystalline phase from phosphatidylcholine at the oil-aqueous interface. *Langmuir.* 21:2804–2810.

34. Hauet, N., F. Artzner, F. Boucher, C. Grabielle-Madelmont, I. Cloutier, G. Keller, P. Lesieur, D. Durand, and M. Paternostre. 2003. Interaction between artificial membranes and enflurane, a general volatile anesthetic: DPPC-enflurane interaction. *Biophys. J.* 84:3123–3137.

35. Schnitzer, E., D. Lichtenberg, and M. Kozov. 2003. Temperature-dependence of the solubilization of dipalmitoylphosphatidylcholine (DPPC) by the non-ionic surfactant Triton X-100, kinetic and structural aspects. *Chem. Phys. Lipids.* 126:55–76.

36. Israelachvili, J. N., D. J. Mitchell, and B. W. Ninham. 1976. Theory of self-assembly of hydrocarbon amphiphiles into micelles and bilayers. *J. Chem. Soc., Faraday Trans. 2.* 72:1525–1568.

37. Lichtenberg, D. 1985. Characterization of the solubilization of lipid bilayers by surfactants. *Biochim. Biophys. Acta.* 821:470–478.

38. Andersson, M., L. Hammarström, and K. Edwards. 1995. Effect of bilayer phase transitions on vesicle structure and its influence on the kinetics of viologen reduction. *J. Phys. Chem.* 99:14531–14538.

39. Mitchell, D. J., and B. W. Ninham. 1981. Micelles, vesicles and microemulsions. *J. Chem. Soc., Faraday Trans. 2.* 77:601–629.

40. Dubois, M., V. Lizunov, A. Meister, T. Gulik-Krzywicki, J. Verbavatz, E. Perez, J. Zimmerberg, and T. Zemb. 2004. Shape control through molecular segregation in giant surfactant aggregates. *Proc. Natl. Acad. Sci. USA.* 101:15082–15087.

41. Johnsson, M., and K. Edwards. 2003. Liposomes, disks, and spherical micelles: aggregates structure in mixtures of gel phase phosphatidylcholines and poly(ethylene glycol)-phospholipids. *Biophys. J.* 85:3839–3847.

42. Vollhardt, D., and V. Fainerman. 2000. Penetration of dissolved amphiphiles into two-dimensional aggregating lipid monolayers. *Adv. Colloid Interface Sci.* 86:103–151.

43. Demel, R. A., W. S. M. Geurts Van Kessel, R. F. A. Zwaal, and B. Roefofsen. 1975. Relation between various phospholipase actions on human red cell membranes and the interfacial phospholipid pressure in monolayers. *Biochim. Biophys. Acta.* 406:97–107.

44. Coutinho, A., and M. Prieto. 2003. Cooperative partition model of nystatin interaction with phospholipid vesicles. *Biophys. J.* 84:3061–3078.

45. Simons, K., and G. van Meer. 1988. Lipid sorting in epithelial cells. *Biochemistry.* 27:6197–6202.

46. Simons, K., and E. Ikonen. 1997. Functional rafts in cell membranes. *Nature.* 387:569–572.

47. Brown, D. A., and E. London. 1998. Structure and origin of ordered lipid domains in biological membranes. *J. Membr. Biol.* 164:103–114.

48. Brown, D. A., and E. London. 1998. Function of lipid rafts in biological membranes. *Annu. Rev. Cell Dev. Biol.* 14:111–136.

49. Parasassi, T., E. Gratton, W. M. Yu, P. Wilson, and M. Levi. 1997. Two-photon fluorescence microscopy of laurdan generalized polarization domains in model and natural membranes. *Biophys. J.* 72: 2413–2429.

50. Filippov, A., G. Orädd, and G. Lindblom. 2006. Sphingomyelin structure influences the lateral diffusion and raft formation in lipid bilayers. *Biophys. J.* 90:2086–2092.

51. Lindblom, G., G. Orädd, and A. Filippov. 2006. Lipid lateral diffusion in bilayers with phosphatidylcholine, sphingomyelin and cholesterol. An NMR study of dynamics and lateral phase separation. *Chem. Phys. Lipids.* 141:179–184.

52. Brown, D. A., and E. London. 2000. Structure and function of sphingolipid-and cholesterol-rich membrane rafts. *J. Biol. Chem.* 275: 17221–17224.

53. Schroeder, R., E. London, and D. Brown. 1994. Interactions between saturated acyl chains confer detergent resistance on lipids and glycosylphosphatidylinositol (GPI)-anchored proteins: GPI-anchored proteins in liposomes and cells show similar behavior. *Proc. Natl. Acad. Sci. USA.* 91:12130–12134.

54. Schroeder, R. J., S. N. Ahmed, Y. Zhu, E. London, D. A. Brown. 1998. Cholesterol and sphingolipid enhance the Triton X-100 insolubility of glycosylphosphatidylinositol-anchored proteins by promoting the formation of detergent-insoluble ordered membrane domains. *J. Biol. Chem.* 273:1150–1157.

55. Pralle, A., P. Keller, E. L. Florin, K. Simons, J. K. H. Horber. 2000. Sphingolipid-cholesterol rafts diffuse as small entities in the plasma membrane of mammalian cells. *J. Cell Biol.* 148:997–1008.

56. Lichtenberg, D., R. J. Robson, and E. A. Dennis. 1983. Solubilization of phospholipids by detergents. Structural and kinetic aspects. *Biochim. Biophys. Acta.* 737:285–304.

57. Vinson, P. K., Y. Talmon, and A. Walter. 1989. Vesicle-micelle transition of phosphatidylcholine and octyl glucoside elucidated by cryo-transmission electron microscopy. *Biophys. J.* 56:669–681.

58. Kragh-Hansen, U., M. Le Maire, and J. V. Moller. 1998. The mechanism of detergent solubilization of liposomes and protein-containing membranes. *Biophys. J.* 75:2932–2946.

59. Deleu, M., O. Bouffioux, H. Razafindralambo, M. Paquot, C. Hbid, P. Thonart, P. Jacques, and R. Brasseur. 2003. Interaction of surfactin with membranes: a computational approach. *Langmuir.* 19:3377–3385.

60. Ickenstein, L. M., M. C. Arfvidsson, D. Needham, L. D. Mayer, and K. Edwards. 2003. Disc formation in cholesterol-free liposomes during phase transition. *Biophys. Biochim. Acta* 1614.:135–138.

61. Sandström, M. C., E. Johansson, and K. Edwards. 2007. Structure of mixed micelles formed in PEG-lipid/lipid dispersions. *Langmuir.* 23: 4192–4198.

62. Funari, S. S., B. Nuscher, G. Rapp, and K. Beyer. 2001. Detergent-phospholipid mixed micelles with a crystalline phospholipid core. *Proc. Natl. Acad. Sci. USA.* 98:8938–8943.

63. Plasencia, I., K. Keough, and J. Perez-Gil. 2005. Interaction of the N-terminal segment of pulmonary surfactant protein SP-C with interfacial phospholipid films. *Biophys. Biochim. Acta.* 1713:118–128.